IEEE Access
Multidisciplinary | Rapid Review | Open Access Journal

Received 16 February 2024, accepted 17 March 2024, date of publication 25 March 2024, date of current version 3 April 2024.

Digital Object Identifier 10.1109/ACCESS.2024.3381518

RESEARCH ARTICLE

The Influence of High Operation Platform Mode on U-Shaped Automated Container Terminal Efficiency

XIAO-JUN LI[1,2,3], RAN ZHOU[1,2], LE-QUN ZHU[1,2], AND YI-SHENG WANG[1,2]

[1]Transport Development Policy Research Center, Tianjin Research Institute for Water Transport Engineering, M.O.T., Tianjin 300456, China
[2]National Engineering Research Center of Port Hydraulic Construction Technology, Tianjin 300456, China
[3]School of Maritime Economics and Management, Dalian Maritime University, Dalian 116026, China

Corresponding author: Le-Qun Zhu (zhulequn@hotmail.com)

This work was supported in part by the National Key Research and Development Program under Grant 2022YFC3203400 and Grant 2022YFE0113500, in part by the Key Research and Development Program under Grant 22YFZCSN00030, and in part by the Research and Innovation Fund under Grant TKS20230408.

ABSTRACT Improving operational efficiency and reducing energy consumption are common objectives for all ports. In previous research by authors, a new high operation platform mode was proposed. It had been proven to reduce energy consumption and be economically feasible. On this basis, this paper studied the influence of high operation platform mode on automated container terminal (ACT) efficiency. This paper took U-shaped ACT as the research object, put forward the operation characteristics of U-shaped ACT under high operation platform mode, and constructed the operation time model of high and low operation platform mode respectively. This paper took 30 containers at the same bay as an example to calculate and verify. The computational results shows that when V_v^1/V_h^1 is above the $V_v^1/V_h^1-\alpha$ curve, the operation time of high platform mode is shorter, and the operation efficiency of ACT is higher (V_v^1 represents the speed of spreader with container vertically moving;V_h^1 represents the speed of spreader with container horizontally moving.); when V_v^1/V_h^1 is under the $V_v^1/V_h^1-\alpha$ curve, the shortening time of quay cranes operation is greater than the increasing time of yard cranes operation, so the overall operational efficiency of ACT is still improved. Therefore, high operation platform mode can improve efficiency of ACT.

INDEX TERMS U-shaped automated container terminal, high operation platform, operation efficiency.

I. INTRODUCTION

The number of containers handled in container terminals has increased astronomically [1]. In order to adapt to this trend, technological innovations in cargo handling equipment have made it possible to automate operational processes in container terminals during the last three decades [2], [3], [4]. As automated container terminal (ACT) technology can improve productive efficiency, reduce energy consumption and cost, a growing number of ACTs have been in operation or construction [5]. Now parallel, perpendicular, and U-shaped layout ACT are three main types of ACT in the world. Perpendicular layout design is implemented in Maasvlakte II ACT in Rotterdam, Yangshan IV ACT in China, and other ACTs worldwide. Tianjin Port in China adopts Parallel layout design. U-shaped layout design is first and only used in Qinzhou Port in China. Since the first ACT was built at Europe Container Terminals Delta Terminal in Port Rotterdam in the year 1993, a lot of research on increasing ACT productive efficiency had been done [6].

As for perpendicular layout ACT, [7] studied the different layout patterns of reefer containers in the yard blocks for effecting on the productivity of ACT in perpendicular layout, and provided the optimal layout of reefer containers in blocks. The results indicated the internal layout of the block as one factors of ACT layout could influence terminal

The associate editor coordinating the review of this manuscript and approving it for publication was Qingchao Jiang.

© 2024 The Authors. This work is licensed under a Creative Commons Attribution-NonCommercial-NoDerivatives 4.0 License.
For more information, see https://creativecommons.org/licenses/by-nc-nd/4.0/

performance. Reference [8] estimated the efficiency of ACT considering various factors. Numerical experiments were conducted to provide management insights into resource optimization. Reference [9] provided the dynamic yard allocation method for improving the performance of ACT in considering the mixed stacking of import and export containers in one block and the cooperation among multiple yard cranes. Reference [10] provided the method of optimization of resource allocation for perpendicular layout, and showed this method how to improve ACT efficiency.

As for parallel layout ACT, [11] designed an isolated lane layout of the yard, which physically separated the automated vehicles from the external trucks while driving. Compared with the perpendicular layout, parallel layout had good performance in the average waiting time of trucks and the operation efficiency of the yard. Reference [12] investigated how the width of the block affect traditional container terminal performance under parallel layout and gave the optimal block width to guide terminal layout design. Reference [13] studied storage block layout and automated yard crane systems on the performance of seaport container terminals under perpendicular layout.

As for U-shaped layout ACT, [14] conducted a detailed simulation research on terminal layout in ACTs from efficiency, economic, and environment perspectives. The results indicated that U-shaped layout design had best performance. Reference [15] provided a hybrid programming model for conflict-free integrated scheduling of quay cranes, AGVs, and double-cantilever rail cranes. The results showed the model could optimize multi-equipment scheduling and improve ACT efficiency. Reference [16] proposed a regional coordinated scheduling strategy considering the energy consumption and efficiency. The result showed it could reduce the conflicts between devices, reduce energy consumption, and improve ACT efficiency. The more papers on improving ACT efficiency can be found in [17] and [18]. Reference [17] made a literature review on yard operations and management in ACT, and discussed the key to improve container handling efficiency based more than 600 papers during the last 20 years. Reference [18] provided a literature review on the global trends of ACT.

These studies were based on parallel, perpendicular, and U-shaped layout, that Intelligent Guided Vehicles (IGVs) and external trucks travelled at the same platform. If IGVs and external trucks travelled at the different platforms, how will the operation efficiency of ACT change? In the previous research by the authors [19], a new high operation platform mode was proposed. It has been proven to reduce energy consumption and be economically feasible. But whether it can improve the ACT efficiency has not been proven. Therefore, we firstly introduced high platform mode and developed respectively operation time models for the high platform mode and the low platform mode based on U-shaped layout ACT (Section II). To verify that the new platform mode can improve operational efficiency, we carried out case calculations (Section III). The results showed that the new mode had good performance on improving U-shaped ACT efficiency. The concrete conclusions and future work are drawn in Section IV.

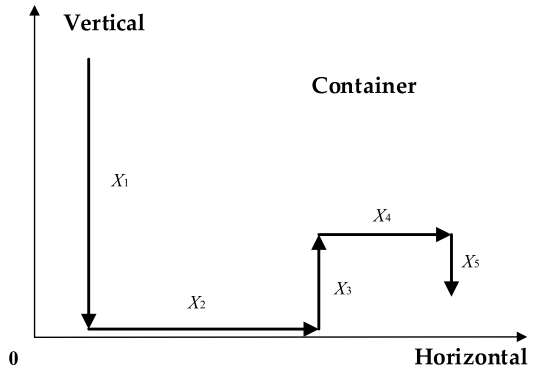

FIGURE 1. Moving route of container under low operation platform mode.

II. METHODOLOGY

A. THE LOW OPERATION PLATFORM AND HIGH OPERATION PLATFORM

The high operation platform mode is a new mode proposed by our research team compared with the low operation platform mode of containers yard. The low operation platform mode means all of the quay cranes, yard cranes, and trucks work on the ground, and x represents the ground (i.e., the low platform). The high operation platform is built above the container yard, and y represents the high operation platform. In high operation platform mode, the quay cranes, storage yard, and external trucks are located in x platform, and the yard cranes and IGVs are located in y platform. The area of y platform located above the containers in the yard is an open rectangle, so that the spreader of the yard crane is able to be lifted and lowered in order to handle containers through this open rectangle [19].

1) MOVING ROUTE OF CONTAINER UNDER LOW OPERATION PLATFORM

The moving route of container from ship side to storage yard under low operation platform mode consists of 5 parts, as shown in the FIGURE 1.

Part 1: The container is vertically lowered onto IGV by quay crane, and X_1 is the corresponding distance of container movement.

Part 2: The container is horizontally transported to the yard by IGV, and X_2 is the corresponding distance of container movement.

Part 3: The container is vertically hoisted to a certain height by yard crane, and X_3 is the corresponding distance of container movement.

Part 4: The container is horizontally moved for a certain distance, and X_4 is the corresponding distance of container movement.

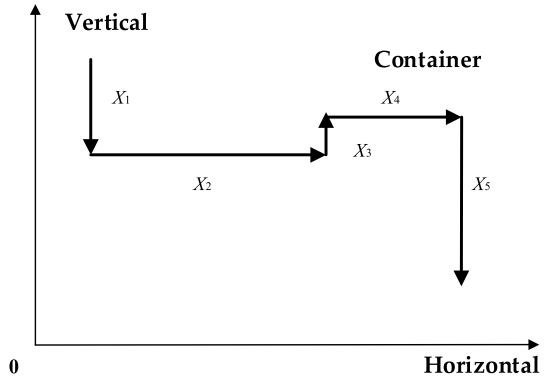

FIGURE 2. Moving route of container under high operation platform mode.

Part 5: The container is vertically lowered to a predetermined position in yard, and X_5 is the corresponding distance of container movement.

2) MOVING ROUTE OF CONTAINER UNDER HIGH OPERATION PLATFORM

The moving route of container from ship side to storage yard under high operation platform mode also consists of 5 parts, as shown in the FIGURE 2. We can see that the container have repeated energy consuming paths in Part 1, Part 3, and Part 5 both FIGURE 1 and FIGURE 2. The length of repeated energy consuming paths is $2X_3$. The difference is that X_3 under high operation platform mode is much smaller than that under low operation platform mode. Because of this difference, [19] proved high operation mode can save energy. However, whether a series of changes in handling and transportation organization caused by this difference can improve ACT operational efficiency will be studied in this paper.

This paper takes U-shaped ACT as the research object and studies the operation time of automated terminal under two modes to determine whether the high platform can improve ACT operation efficiency. The theoretical models are developed based on the process of handling 30 importing containers. The process is to unload 30 containers from the ship to the same bay of the yard (6 rows and 5 tiers), and we called this process as ''yard containers loading process'', and then the 30 containers are removed from the yard by an external truck, and we called this process as ''yard containers unloading process''. In this paper, the unit of distance is meter, the unit of time is second.

B. ASSUMPTIONS OF THE MODEL

The assumptions are as follows:

1) All 30 containers are 20ft standard containers.

2) All 30 containers are the same on weight.

2) The yard crane is bilateral-cantilever automated rail-mounted gantry crane.

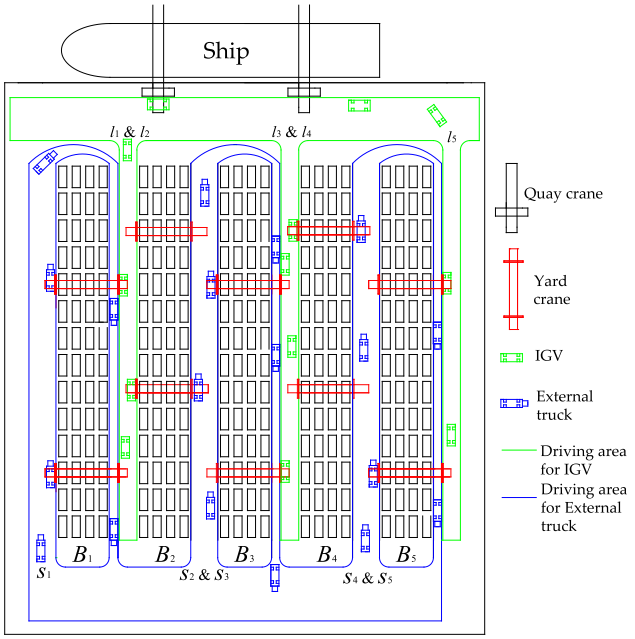

FIGURE 3. Layout of x platform in low operation platform mode.

4) The spreader keeps a constant speed at the same stage. The upward motion speed of the container hoisted by the spreader is the same as the downward motion speed of the container lowered by the spreader. The upward motion speed of the spreader without container is the same as the downward motion speed of the spreader without container.

5) The sequence in which containers are unloaded from the ship to the yard is the opposite of the sequence in which containers are removed from the yard.

6) The initial position of the yard crane spreader is located above the container truck.

C. THE TIME MODEL OF LOW OPERATION PLATFORM FOR U-SHAPED ACT

FIGURE 3 shows the layout of x platform in low operation platform mode. IGV can travel in both directions. When IGV travels in the yard interior roads l_1,l_2,l_3,l_4,l_5, IGV does not need to turn 180 degrees. B_1, B_2,B_3,B_4,B_5 are five container blocks. S_1, S_2,S_3,S_4,S_5 are U-shaped routes. Taking S_2,S_3 for example, left channel of U-shaped route is located outside the yard crane track, and right channel is located inside the yard crane track. Although S_2 and S_3 share the same road between B_2 and B_3, the service area is different. For S_2, external trucks complete the loading and unloading of containers in B_2 at left channel, and leave yard through the right channel. While for S_3, external trucks complete the loading and unloading of containers in B_3 at left channel, and leave yard through the right channel.

The process for containers handling under low operation platform mode have two part, yard containers loading process (L-1) and yard containers unloading process (L-2).

1) YARD CONTAINERS LOADING PROCESS UNDER LOW OPERATION PLATFORM MODE (L-1)

The entire process of container i loading and unloading by yard crane spreader in L-1 consists of six stages.

Stage 1: The yard crane spreader vertically lowers to hoist container i. The time, distance, and speed of spreader running are t_i^1, d_i^1, v_i^1 respectively.

Stage 2: The yard crane spreader vertically hoists container i to a certain height. The time, distance, and speed of spreader running are t_i^2, d_i^2, v_i^2 respectively.

Stage 3: The yard crane spreader with container i horizontally moves for a certain distance. The time, distance, and speed of spreader running are t_i^3, d_i^3, v_i^3 respectively.

Stage 4: The yard crane spreader vertically lowers container i to predetermined position. The time, distance, and speed of spreader running are t_i^4, d_i^4, v_i^4 respectively.

Stage 5: The yard crane spreader vertically hoists to a certain height. The time, distance, and speed of spreader running are t_i^5, d_i^5, v_i^5 respectively.

Stage 6: The yard crane spreader horizontally moves for a certain distance to prepare to hoist container $i+1$. The time, distance, and speed of spreader running are t_i^6, d_i^6, v_i^6 respectively.

The time of yard crane spreader running in L-1 (T_L^1) can be calculated as follows.

$$T_L^1 = \sum\nolimits_i \left(t_i^1 + t_i^2 + t_i^3 + t_i^4 + t_i^5 + t_i^6\right) \tag{1}$$

Based on assumption (4), we can get (2).

$$T_L^1 = \sum\nolimits_i \left(\frac{d_i^1}{v_i^1} + \frac{d_i^2}{v_i^2} + \frac{d_i^3}{v_i^3} + \frac{d_i^4}{v_i^4} + \frac{d_i^5}{v_i^5} + \frac{d_i^6}{v_i^6}\right) \tag{2}$$

2) YARD CONTAINERS UNLOADING PROCESS UNDER LOW OPERATION PLATFORM MODE (L-2)

The entire process of container j loading and unloading by yard crane spreader in L-2 consists of six stages.

Stage 1: The yard crane spreader horizontally moves for a certain distance to prepare to hoist container j. The time, distance, and speed of spreader running are t_j^{11}, d_j^{11}, v_j^{11} respectively.

Stage 2: The yard crane spreader vertically lowers to hoist container j. The time, distance, and speed of spreader running are t_j^{12}, d_j^{12}, v_j^{12} respectively.

Stage 3: The yard crane spreader vertically hoists container j to a certain height. The time, distance, and speed of spreader running are t_j^{13}, d_j^{13}, v_j^{13} respectively.

Stage 4: The yard crane spreader with container j horizontally moves for a certain distance. The time, distance, and speed of spreader running are t_j^{14}, d_j^{14}, v_j^{14} respectively.

Stage 5: The yard crane spreader vertically lowers container j to predetermined position. The time, distance, and speed of spreader running are t_j^{15}, d_j^{15}, v_j^{15} respectively.

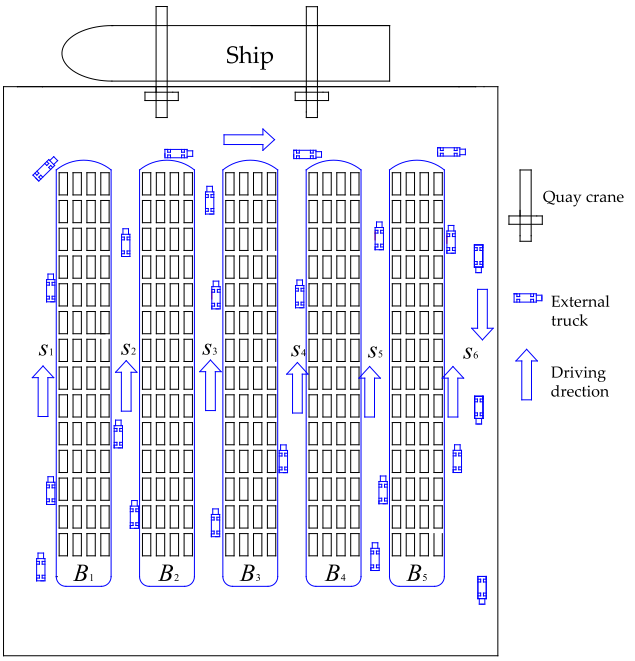

FIGURE 4. Layout of x platform in high operation platform mode.

Stage 6: The yard crane spreader vertically hoists to a certain height. The time, distance, and speed of spreader running are t_j^{16}, d_j^{16}, v_j^{16} respectively.

The time of yard crane spreader running in L-2 (T_L^2) can be calculated as follows.

$$T_L^2 = \sum\nolimits_j \left(t_j^{11} + t_j^{12} + t_j^{13} + t_j^{14} + t_j^{15} + t_j^{16}\right) \tag{3}$$

Based on assumption (4), we can get (4).

$$T_L^2 = \sum\nolimits_j \left(\frac{d_j^{11}}{v_j^{11}} + \frac{d_j^{12}}{v_j^{12}} + \frac{d_j^{13}}{v_j^{13}} + \frac{d_j^{14}}{v_j^{14}} + \frac{d_j^{15}}{v_j^{15}} + \frac{d_j^{16}}{v_j^{16}}\right) \tag{4}$$

The time of yard crane spreader running in low operation platform mode (T_L) can be calculated as follows.

$$T_L = \sum\nolimits_i \left(\frac{d_i^1}{v_i^1} + \frac{d_i^2}{v_i^2} + \frac{d_i^3}{v_i^3} + \frac{d_i^4}{v_i^4} + \frac{d_i^5}{v_i^5} + \frac{d_i^6}{v_i^6}\right) + \sum\nolimits_j \left(\frac{d_j^{11}}{v_j^{11}} + \frac{d_j^{12}}{v_j^{12}} + \frac{d_j^{13}}{v_j^{13}} + \frac{d_j^{14}}{v_j^{14}} + \frac{d_j^{15}}{v_j^{15}} + \frac{d_j^{16}}{v_j^{16}}\right) \tag{5}$$

D. THE TIME MODEL OF HIGH OPERATION PLATFORM FOR U-SHAPED ACT

FIGURE 4 shows the layout of x platform in high operation platform mode.

In the high operation platform mode, external trucks complete the collection and distribution of yard containers with the help of yard cranes at x platform. Compared with

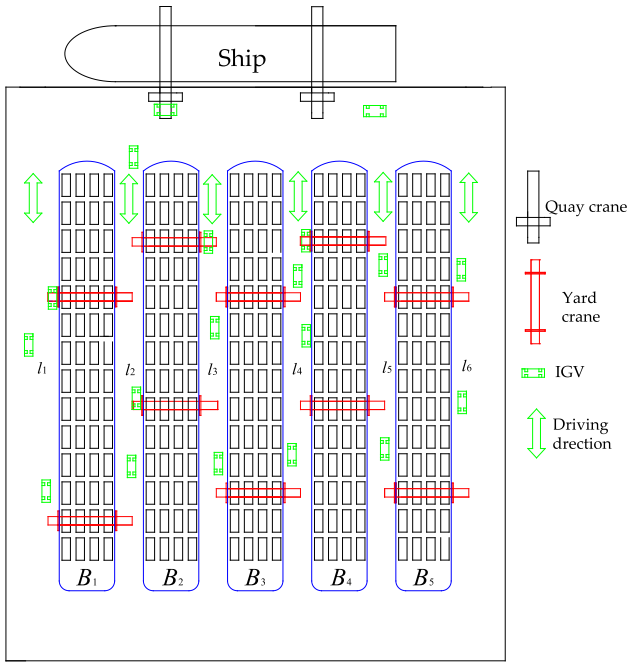

FIGURE 5. Layout of y platform in high operation platform mode.

U-shaped yard under low operation platform mode, the main characteristics of high operation platform mode at x platform are as follows.

1) Only external trucks run at x platform, so IGVs and external trucks do not meet.

2) There is a one-way external trucks lane between every two blocks.

3) Each bay can be loaded and unloaded on both sides, while the low operation platform can only be loaded and unloaded on one side for external trucks.

The operation of containers from ship to yard, and from yard to external trucks are completed at y platform (FIGURE 5). Compared with U-shaped yard under low operation platform, the main characteristics of high operation platform mode at y platform are as follows.

1) Only IGVs run at y platform, so IGVs and external trucks do not meet.

2) Each bay can be loaded and unloaded on both sides, while the low operation platform mode can only be loaded and unloaded on one side for IGVs.

3) In the process of yard crane moving containers to yards, all containers are handling on high platforms, so when spreader with container carries out transverse operation, the height of containers being crossed will hardly affect the crossing operation.

The process for containers handling under high operation platform mode have two parts, yard containers loading process (H-1) and yard containers unloading process (H-2).

1) YARD CONTAINERS LOADING PROCESS UNDER HIGH OPERATION PLATFORM MODE (H-1)

The stages of container *i*handling with yard crane in high and low operation platform mode is roughly the same. The entire process also consists of six stages in H-1. The time, distance, and speed of spreader running are T_i^1, D_i^1, V_i^1respectively at Stage 1 in H-1, which are similar to those in L-1, so do Stage 2-6. The difference is that container truck can unload container on both sides of Block in H-1. The container trucks will operate at the channel that is closer to the container.

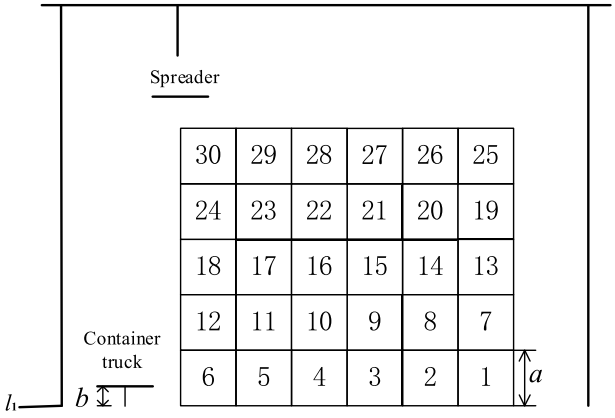

FIGURE 6. Yard containers operation sequence in L-1.

The time of yard crane spreader running in H-1 (T_H^1) can be calculated as follows.

$$T_H^1 = \sum\nolimits_i \left(T_i^1 + T_i^2 + T_i^3 + T_i^4 + T_i^5 + T_i^6\right) \tag{6}$$

Based on assumption (4), we can get (7).

$$T_H^1 = \sum\nolimits_i \left(\frac{D_i^1}{V_i^1} + \frac{D_i^2}{V_i^2} + \frac{D_i^3}{V_i^3} + \frac{D_i^4}{V_i^4} + \frac{D_i^5}{V_i^5} + \frac{D_i^6}{V_i^6}\right) \tag{7}$$

2) YARD CONTAINERS UNLOADING PROCESS UNDER HIGH OPERATION PLATFORM MODE (H-2)

The stages of container *j*handling with yard crane in high and low operation platform mode is roughly the same. The entire process also consists of six stages in H-2. The time, distance, and speed of spreader running are T_j^{11}, D_j^{11}, V_j^{11}respectively at Stage 1 in H-2, which are similar to those in L-2, so do Stage 2-6. The difference is also that container truck can unload container on both sides of Block in H-2.

The time of yard crane spreader running in H-2 (T_H^2) can be calculated as follows.

$$T_H^2 = \sum\nolimits_j \left(T_j^{11} + T_j^{12} + T_j^{13} + T_j^{14} + T_j^{15} + T_j^{16}\right) \tag{8}$$

Based on assumption (4), we can get (9).

$$T_H^2 = \sum\nolimits_j \left(\frac{D_i^{11}}{V_j^{11}} + \frac{D_i^{12}}{V_j^{12}} + \frac{D_i^{13}}{V_j^{13}} + \frac{D_i^{14}}{V_j^{14}} + \frac{D_i^{15}}{V_j^{15}} + \frac{D_i^{16}}{V_j^{16}}\right) \tag{9}$$

The time of yard crane spreader running in high operation platform mode (T_H) can be calculated as follows.

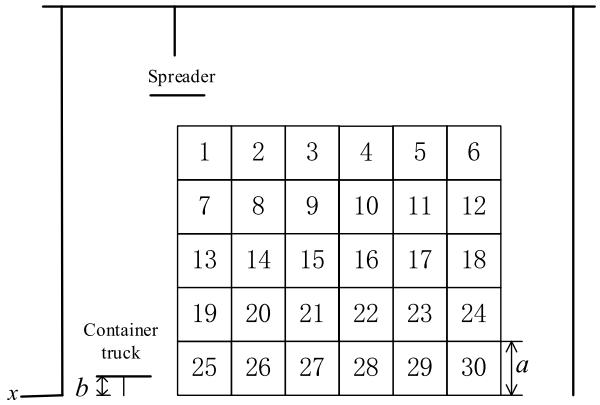

FIGURE 7. Yard containers operation sequence in L-2.

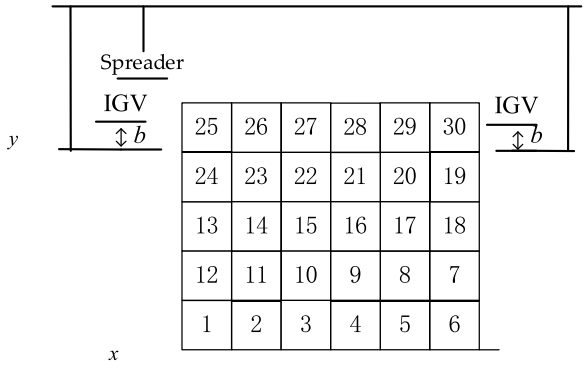

FIGURE 8. Yard containers operation sequence in H-1.

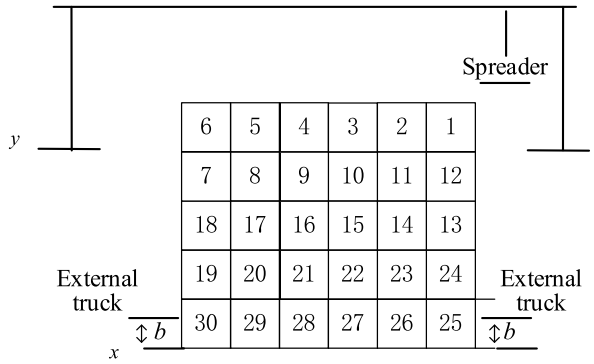

FIGURE 9. Yard containers operation sequence in H-2.

$$T_H = \sum_i \left(\frac{D_i^1}{V_i^1} + \frac{D_i^2}{V_i^2} + \frac{D_i^3}{V_i^3} + \frac{D_i^4}{V_i^4} + \frac{D_i^5}{V_i^5} + \frac{D_i^6}{V_i^6} \right) + \sum_j \left(\frac{D_i^{11}}{V_j^{11}} + \frac{D_i^{12}}{V_j^{12}} + \frac{D_i^{13}}{V_j^{13}} + \frac{D_i^{14}}{V_j^{14}} + \frac{D_i^{15}}{V_j^{15}} + \frac{D_i^{16}}{V_j^{16}} \right) \tag{10}$$

III. CALCULATION AND ANALYSIS

A. EXAMPLE DESCRIPTION

Yard containers are stacked in 5 tiers. The height of x platform is 0 meter (H_x= 0). The height of y platform is 4a (H_y= 4a),

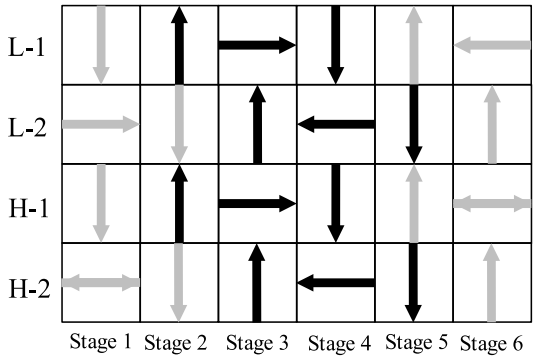

FIGURE 10. The spreader movement of the six stages in L-1, L-2, H-1, H-2.

TABLE 1. The distance of the spreaders are got at stage 1 in l-1.

i	d_i^1	i	d_i^1
1	h	16	2a-b+h
2	h	17	2a-b+h
3	h	18	2a-b+h
4	h	19	2a-b+h
5	h	20	3a-b+h
6	h	21	3a-b+h
7	h	22	3a-b+h
8	a-b+h	23	3a-b+h
9	a-b+h	24	3a-b+h
10	a-b+h	25	3a-b+h
11	a-b+h	26	4a-b+h
12	a-b+h	27	4a-b+h
13	a-b+h	28	4a-b+h
14	2a-b+h	29	4a-b+h
15	2a-b+h	30	4a-b+h

and a is the height of a 20ft standard container. b is the height of the container truck platform. c is the width of a 20ft standard container. When spreader (or spreader with container) carries out transverse operation, the vertical distance between the bottom of spreader (or container hoisted by spreader) and the top of container being crossed can be a fixed height h.

1) YARD CONTAINERS OPERATION SEQUENCE

The yard containers operation sequences in L-1, L-2, H-1, H-2 are shown in FIGURE 6, FIGURE 7, FIGURE 8, FIGURE 9 respectively.

2) SPEED OF SPREADER

The spreader movement displacement diagram of the six stages in L-1, L-2, H-1, H-2 is shown in FIGURE 10. In FIGURE 10, the black arrow indicates that the spreader is hoisting the container, the gray arrow indicates that the spreader is unloaded, the arrow indicates the direction, and the two-way arrow indicates that the spreader moves in different directions for different containers at this stage.

Based on assumption (1), (2), (4), we can get (11)–(14).

$$v_i^1 = v_i^5 = v_j^{12} = v_j^{16} = V_j^1 = V_j^5 = V_j^{12} = V_j^{16} = V_v^0 \tag{11}$$

$$v_i^2 = v_i^4 = v_j^{13} = v_j^{15} = V_j^2 = V_j^4 = V_j^{13} = V_j^{15} = V_v^1 \tag{12}$$

TABLE 2. The distance of the spreaders are got at each stage.

Stage	L-1	L-2	H-1	H-2
Stage 1	56*a*-23*b*+30*h*	105*c*	30*h*	78*c*
Stage 2	60*a* -24*b*+30*h*	6*b*+30*h*	30*h*	6*b*+30*h*
Stage 3	105*c*	6*b*+30*h*	72*c*	6*b*+30*h*
Stage 4	6*b*+30*h*	105*c*	60*a*+30*b*+30*h*	78*c*
Stage 5	6*b*+30*h*	60*a* -24*b*+30*h*	60*a*+30*b*+30*h*	60*a*-24*b*+30*h*
Stage 6	105*c*	56*a*-23*b*+30*h*	78*c*	56*a*-23*b*+30*h*

$$v_i^6 = v_j^{11} = V_j^6 = V_j^{11} = V_h^0 \tag{13}$$
$$v_i^3 = v_j^{14} = V_j^3 = V_j^{14} = V_h^1 \tag{14}$$

V_v^0 represents the speed of spreader vertically moving.
V_v^1 represents the speed of spreader with container vertically moving.
V_h^0 represents the speed of spreader horizontally moving.
V_h^1 represents the speed of spreader with container horizontally moving.

B. MODEL CALCULATION

According to the operation sequence of completing 30 containers, the distance of the spreaders can be got at each stage. TABLE 1 shows the distances of the spreaders for 30 containers (d_i^1) at Stage 1 in L-1. We calculated the distance of the spreaders at each stage in each process one by one as the work in TABLE 1, then we got TABLE 2.

Taking the values in TABLE 2 into (5) and (10), So we can get T_L, T_H as (15) and (16).

$$\begin{aligned} T_L = {} & \frac{56a-23b+30h}{V_v^0} + \frac{60a-24b+30h}{V_v^1} + \frac{105c}{V_h^1} \\ & + \frac{6b+30h}{V_v^1} + \frac{6b+30h}{V_v^0} + \frac{105c}{V_h^0} \\ & + \frac{105c}{V_h^0} + \frac{6b+30h}{V_v^0} + \frac{6b+30h}{V_v^1} + \frac{105c}{V_h^1} \\ & + \frac{60a-24b+30h}{V_v^1} + \frac{56a-23b+30h}{V_v^0} \end{aligned} \tag{15}$$

$$\begin{aligned} T_H = {} & \frac{30h}{V_v^0} + \frac{30h}{V_v^1} + \frac{72c}{V_h^1} + \frac{60a+30b+30h}{V_v^1} \\ & + \frac{60a+30b+30h}{V_v^0} + \frac{78c}{V_h^0} + \frac{78c}{V_h^0} \\ & + \frac{6b+30h}{V_v^0} + \frac{6b+30h}{V_v^1} + \frac{78c}{V_h^1} + \frac{60a-24b+30h}{V_v^1} \\ & + \frac{56a-23b+30h}{V_v^0} \end{aligned} \tag{16}$$

Taking (11)- (14) in (15) and (16), we have (17) and (18).

$$\begin{aligned} T_L = {} & \frac{112a-34b+120h}{V_v^0} + \frac{120a-36b+120h}{V_v^1} \\ & + \frac{210c}{V_h^0} + \frac{210c}{V_h^1} \end{aligned} \tag{17}$$

$$\begin{aligned} T_H = {} & \frac{116a+13b+120h}{V_v^0} + \frac{120a+12b+120h}{V_v^1} \\ & + \frac{156c}{V_h^0} + \frac{150c}{V_h^1} \end{aligned} \tag{18}$$

The difference in time consumption between the two modes (ΔT) can be calculated as (19).

$$\Delta T = T_H - T_L = \frac{4a+47b}{V_v^0} + \frac{48b}{V_v^1} - \frac{54c}{V_h^0} - \frac{60c}{V_h^1} \tag{19}$$

TABLE 3 shows the values of the relevant parameters. Taking the values in TABLE 3 in (19), then we have:

$$\Delta T = \frac{80.86}{V_v^0} + \frac{72}{V_v^1} - \frac{131.652}{V_h^0} - \frac{146.28}{V_h^1} \tag{20}$$

TABLE 3. The values of the relevant parameters.

Parameters	*a*	*b*	*c*	*h*
Numerical values	2.59 m	1.5 m	2.438 m	0.3 m

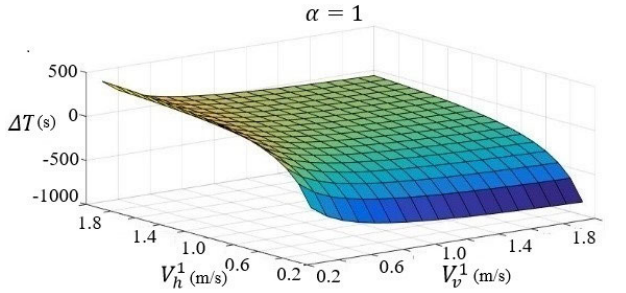

FIGURE 11. α =1, X-Y-Z view.

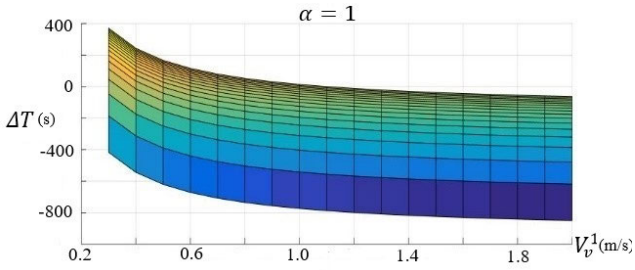

FIGURE 12. α =1, X-Z view.

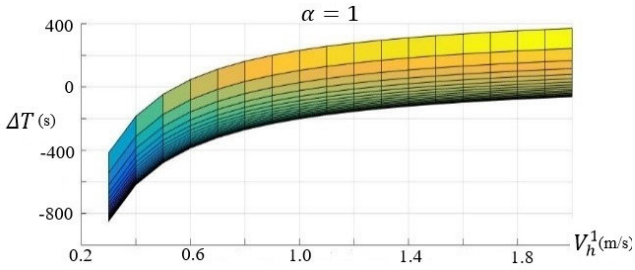

FIGURE 13. α =1, Y-Z view.

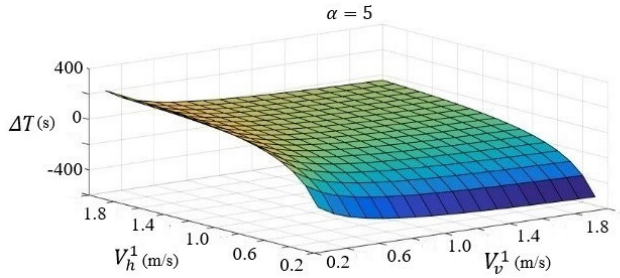

FIGURE 14. α =5, X-Y-Z view.

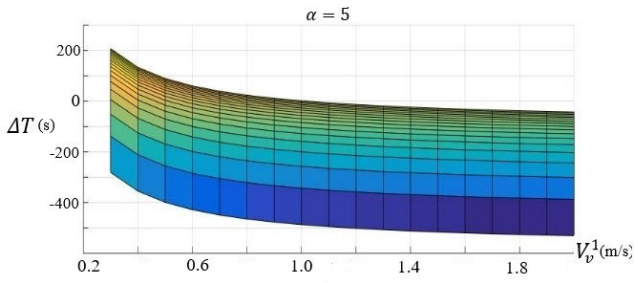

FIGURE 15. α =5, X-Z view.

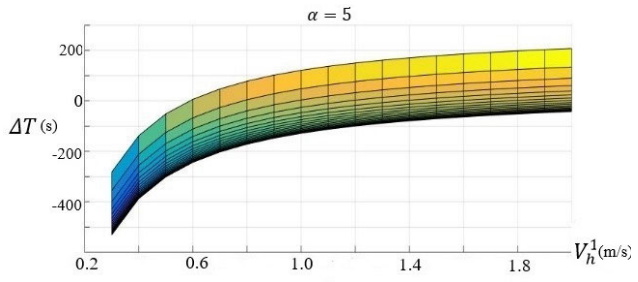

FIGURE 16. α =5, Y-Z view.

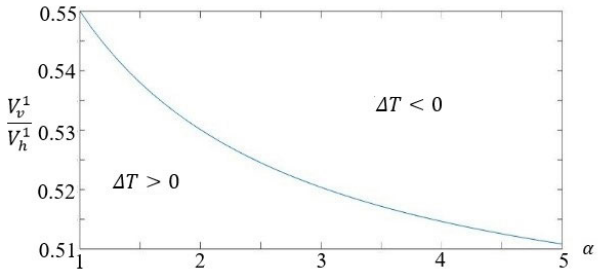

FIGURE 17. Relationship curve of $V_v^1/V_h^1-\alpha$.

Assuming that the speed of spread without container is α times the speed of spread with container($1 \leq \alpha \leq 5$), then we have:

$$V_v^0 = \alpha V_v^1 \tag{21}$$

$$V_h^0 = \alpha V_h^1 \tag{22}$$

Taking (21) and (22) in (20), then we have:

$$\Delta T = \frac{80.86}{\alpha V_v^1} + \frac{72}{V_v^1} - \frac{131.652}{\alpha V_h^1} - \frac{146.28}{V_h^1} \tag{23}$$

We take two boundary values $\alpha = 1$ and $\alpha = 5$ respectively to generate three-dimensional graphs, as shown in FIGURE 11-FIGURE 16. It can be seen from the figure (especially in X-Z view and Y-Z view) that ΔT has an interval greater than zero. $\Delta T > 0$ indicates that the operation time of the yard crane in high platform mode is longer than that in low platform mode.

We further calculate (23) to get (24) under $\Delta T > 0$.

$$\frac{V_v^1}{V_h^1} \leq \frac{80.86 + 72\alpha}{131.652 + 146.28\alpha} \tag{24}$$

The relationship between$V_v^1/V_h^1$and α is shown in FIGURE 17. For different values of α, When V_v^1/V_h^1 is above the $V_v^1/V_h^1 - \alpha$ curve ($\Delta T < 0$), the operation time of high operation platform mode is shorter, and the operation efficiency of ACT is higher. When V_v^1/V_h^1 is under the $V_v^1/V_h^1 - \alpha$ curve ($\Delta T > 0$), the operation time of high operation platform mode is longer and the operation efficiency of the yard is reduced. However, to evaluate the overall efficiency of ACT, it is necessary to compare the shortened value of quay crane operation with the added value of yard operation.

Compared with low operation platform mode, the vertical motion distance of the quay crane spreader handling 30 containers is reduced by ΔH_Q under high operation platform mode.

$$\Delta H_Q = 30 \cdot 2\left(H_y - H_x\right) = 240a \tag{25}$$

The quay crane spreader moves up and down the same distance of $120a$. V_1 and αV_1 are speeds of spread with container and spread of quay crane. Assuming that $V_1 = V_v^1$, then we have:

$$\Delta T_Q = \frac{120a}{V_v^1} + \frac{120a}{\alpha V_v^1} \tag{26}$$

$$\Delta T_{ACT} = \Delta T_Q - \Delta T \tag{27}$$

ΔT_Q represents the difference in operating time of quay crane between high operation platform mode and low operation platform mode.

ΔT_{ACT} represents the shortened value of quay crane operation minus the added value of yard operation. Because quay crane operation efficiency is bottleneck of container port and yard crane operation efficiency can be improved by increasing the number of yard crane operating at the same time, $\Delta T_{ACT} > 0$ means that the efficiency of ACT improves.

Taking (23) and (26) in (27), then we have:

$$\Delta T_{ACT} = \frac{120\alpha a - 48\alpha b + 116a - 47b}{V_v^0} + \frac{54c + 60\alpha c}{V_h^0} \tag{28}$$

Taking the values in TABLE 3 in (28), we have (29).

$$\Delta T_{ACT} = \frac{238.8\alpha + 229.94}{V_v^0} + \frac{131.652 + 146.28\alpha}{V_h^0} \tag{29}$$

As the values of α, V_v^0, and V_h^0 are all greater than 0, $T_{ACT} > 0$. The shortening time of quay cranes operation is greater than the increasing time of yard cranes operation, so it can also improve the overall operational efficiency of ACT under high operation platform mode.

So under high operation platform mode we have:

When $\Delta T < 0$, the operation time of quay cranes and yard cranes is reduced, and the overall operation efficiency of ACT is improved. When $\Delta T > 0$, the shortening time of quay cranes operation is greater than the increasing time of yard cranes operation, so the overall operational efficiency of ACT is still improved. From what has been discussed above, high operation platform mode can improve operational efficiency of ACT.

IV. CONCLUSION AND FUTURE WORK

This paper is an extension of the author's previous research by authors. In this paper, we studied the influence of high operation platform mode on U-shaped ACT efficiency. The major contributions are as follows.

1) The high operation platform mode can optimize U-shaped ACT operation. IGVs run at y platform, and external trucks run at x platform, so IGVs and external trucks do not meet. It will significantly reduce the difficulty of IGVs operation control and improve the efficiency of external trucks. In the high operation platform mode, each containers bay can be loaded and unloaded on both sides by IGVs or external trucks. While the low operation platform mode can only be loaded on one side, which means that yard crane spreader will run a longer distance to complete the containers loading and unloading operation under the low platform mode. In the process of yard crane moving containers to yards, all containers are handling on high operation platforms, so when spreader with container carries out transverse operation, the height of containers being crossed will hardly affect the crossing operation.

2) The high operation platform mode can improve U-shaped ACT operation efficiency. This paper takes 30 imported containers at the same bay as an example to calculate and verify. The computational results shows that when V_v^1/V_h^1 is above the $V_v^1/V_h^1 - \alpha$ curve, the operation time of high platform mode is shorter, and the operation efficiency of ACT is higher; when V_v^1/V_h^1 is under the $V_v^1/V_h^1 - \alpha$ curve, the shortening time of quay cranes operation is greater than the increasing time of yard cranes operation, so the overall operational efficiency of ACT is still improved. Therefore, high operation platform mode can improve operational efficiency of ACT.

There are some possibilities for further research. Firstly, the research primarily relies on theoretical models and computational simulations. In future study, with the normal operation of U-shaped ACTs in China's Qinzhou port, real-world empirical data will be available and provide more robust validation of the proposed model. Secondly, this study focuses on the influence of high operation platform mode on U-shaped ACT efficiency. For parallel and perpendicular layout ACTs, the loading and unloading organization are different from U-shaped ACTs. In future study, we will study the influence of high operation platform mode on parallel and perpendicular layout ACTs. Thirdly, this study does not examine the impact of this high operation platform mode on other aspects such as safety, scalability, and environmental impact. In future study, it is worth to make a comprehensive assessment of the model's impact on safety, scalability and environmental sustainability and cost-effectiveness.

REFERENCES

[1] A. Gharehgozli, N. Zaerpour, and R. de Koster, "Container terminal layout design: Transition and future," *Maritime Econ. Logistics*, vol. 22, no. 4, pp. 610–639, Oct. 2019.

[2] P. Wang, J. P. Mileski, and Q. Zeng, "Alignments between strategic content and process structure: The case of container terminal service process automation," *Maritime Econ. Logistics*, vol. 21, no. 4, pp. 543–558, Dec. 2019.

[3] L. Yue, H. Fan, and C. Zhai, "Joint configuration and scheduling optimization of a dual-trolley quay crane and automatic guided vehicles with consideration of vessel stability," *Sustainability*, vol. 12, no. 1, p. 24, Dec. 2019.

[4] C. Tan, W. Yan, and J. Yue, "Quay crane scheduling in automated container terminal for the trade-off between operation efficiency and energy consumption," *Adv. Eng. Informat.*, vol. 48, Apr. 2021, Art. no. 101285.

[5] M. Wei, J. He, C. Tan, J. Yue, and H. Yu, "Quay crane scheduling with time windows constraints for automated container port," *Ocean Coastal Manage.*, vol. 231, Jan. 2023, Art. no. 106401.

[6] R. Yang and Q. Li, "Research on the system technology for automated container terminal," in *Proc. 29TH Chin. Control Decis. Conf.*, Chongqing, China, 2017, pp. 3463–3466.

[7] C. H. Rim, P. B. Joo, and K. H. Kyoung, "A simulation of optimal layout type of reefer containers in automated container terminal," *WSEAS Trans. Inf. Sci. Appl.*, vol. 3, pp. 2525–2531, Dec. 2006.

[8] X. Xiang, C. Liu, L. H. Lee, and E. P. Chew, "Performance estimation and design optimization of a congested automated container terminal," *IEEE Trans. Autom. Sci. Eng.*, vol. 19, no. 3, pp. 2437–2449, Jul. 2022.

[9] J. He, X. Xiao, and H. Yu, "Dynamic yard allocation for automated container terminal," *Ann. Oper. Res.*, vol. 1, pp. 1–22, Jan. 2022.

[10] X. Zhang, H. Li, and M. Wu, "Optimization of resource allocation in automated container terminals," *Sustainability*, vol. 14, no. 24, p. 16869, Dec. 2022.

[11] Y. Xu, Y. Zhang, P. Chen, R. Yang, and Y. Gao, "Simulation analysis of isolated lane layout in automated container terminal yard," in *Proc. 6th Int. Conf. Transp. Inf. Saf. (ICTIS)*, Wuhan, China, Oct. 2021, pp. 1414–1418.

[12] M. E. H. Petering, "Effect of block width and storage yard layout on marine container terminal performance," *Transp. Res. E, Logistics Transp. Rev.*, vol. 45, no. 4, pp. 591–610, Jul. 2009.

[13] N. Kemme, "Effects of storage block layout and automated yard crane systems on the performance of seaport container terminals," *OR Spectr.*, vol. 34, no. 3, pp. 563–591, Jul. 2012.

[14] X. Li, Y. Peng, J. Huang, W. Wang, and X. Song, "Simulation study on terminal layout in automated container terminals from efficiency, economic and environment perspectives," *Ocean Coastal Manage.*, vol. 213, Nov. 2021, Art. no. 105882.

[15] B. Xu, D. Jie, J. Li, Y. Zhou, H. Wang, and H. Fan, "A hybrid dynamic method for conflict-free integrated schedule optimization in U-Shaped automated container terminals," *J. Mar. Sci. Eng.*, vol. 10, no. 9, p. 1187, Aug. 2022.

[16] Y. Niu, F. Yu, H. Yao, and Y. Yang, "Multi-equipment coordinated scheduling strategy of U-shaped automated container terminal considering energy consumption," *Comput. Ind. Eng.*, vol. 174, Dec. 2022, Art. no. 108804.

[17] H. Yu, Y. Deng, L. Zhang, X. Xiao, and C. Tan, "Yard operations and management in automated container terminals: A review," *Sustainability*, vol. 14, no. 6, p. 3419, Mar. 2022.

[18] W. K. Kon, N. S. F. A. Rahman, R. M. Hanafiah, and S. A. Hamid, "The global trends of automated container terminal: A systematic literature review," *Maritime Bus. Rev.*, vol. 6, no. 3, pp. 206–233, Sep. 2021.
[19] X. Li, R. Zhou, and L. Zhu, "The influence of operation platform on the energy consumption of container handling," *Sustainability*, vol. 15, no. 1, p. 385, Dec. 2022.

XIAO-JUN LI was born in Weihai, Shandong, China, in 1988. He received the B.S., M.S., and Ph.D. degrees in transportation planning and management from Dalian Maritime University, Dalian. From 2016 to 2018, he was an Engineer with the Policy Research Office in TIWTE. Since 2019, he has been a Senior Engineer. He is the author of five books and more than 25 articles. His research interests include maritime transport safety, transportation planning, and management. He was a member of New Think Tank for Transportation.

RAN ZHOU was born in Jingzhou, Hubei, China, in 1981. She received the B.S. degree in environmental science and technology from Yangtze University, Jingzhou, in 2002, the M.S. degree in environmental science and technology from China Agricultural University, Beijing, in 2005, and the Ph.D. degree in environmental science and technology from Sichuan Agricultural University, Chengdu, in 2015. From 2005 to 2016, she was a Senior Engineer with the Princeton Waterway Transportation Environmental Protection Technology Transportation Industry Key Laboratory. Since 2016, she has been the Vice Director of Policy Research Office in TIWTE. She is the author of 14 books, more than 50 articles, and more than 70 projects. Her research interests include environmental protection in transportation and energy conservation and emission reduction. She was a member of Tianjin Belt and Road Expert Database and a member of the Qingdao Shipping Advisory Group.

LE-QUN ZHU was born in Lianyungang, Jiangsu, China, in 1990. He received the B.S., M.S., and Ph.D. degrees in transportation planning and management from Dalian Maritime University, Dalian. From 2016 to 2018, he was a Research Assistant with the Policy Research Office in TIWTE. Since 2019, he has been an Assistant Professor. He is the author of three books and more than 18 articles. His research interests include shipping economics supply-chain management and the safety of sea lines of communication. He was a member of the International Association of Maritime Economics and a member of New Think Tank for Transportation.

YI-SHENG WANG was born in Rizhao, Shandong, China, in 1991. He received the B.S. and M.S. degrees in transport engineering from Beijing Jiaotong University, Beijing.

From 2018 to 2019, he was a Research Intern with the Policy Research Office in TIWTE. Since 2020, he has been a Research Assistant. He is the author of one book and more than 11 articles. His research interests include multimodal transport, maritime supervision, and services. He was a member of New Think Tank for Transportation.